Reliability updating for lateral failure of historic quay walls

Hemel, Mart Jan; Peters, Dirk Jan; Schweckendiek, Timo; Jonkman, Sebastiaan N.
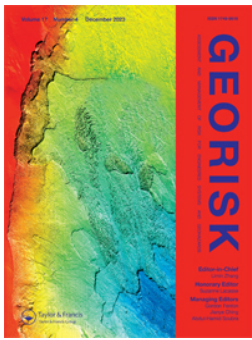
Important note
To cite this publication, please use the final published version (if applicable).
Please check the document version above.

Reliability updating for lateral failure of historic quay walls

Mart-Jan Hemel, Dirk Jan Peters, Timo Schweckendiek & Sebastiaan N. Jonkman

Published online: 09 Jan 2024.

Submit your article to this journal ⏎

Article views: 154

View related articles ⏎

View Crossmark data ⏎

Taylor & Francis
Taylor & Francis Group

Reliability updating for lateral failure of historic quay walls

Mart-Jan Hemel[a,b], Dirk Jan Peters[a,c], Timo Schweckendiek[a,d] and Sebastiaan N. Jonkman[a]

[a]Department of Hydraulic Engineering, Delft University of Technology, Delft, The Netherlands; [b]Amsterdam Institute for Advanced Metropolitan Solutions, Amsterdam, The Netherlands; [c]Department of Maritime, Royal HaskoningDHV, Rotterdam, The Netherlands; [d]Deltares, Deltares Software Centre, Delft, The Netherlands

ABSTRACT

The historic canal walls of Amsterdam, stretching 200 km in total, are constructed as a masonry wall on a timber deck supported by vertical timber piles. Understanding the resistance against lateral failure of these quays has been challenging due to uncertainties in their working principles, geometry, soil and structural properties. This paper proposes a Bayesian approach to include evidence from past loading situations and corresponding deformations into the reliability assessment. This approach enables refinement of the reliability predictions and parameter distribution uncertainties, leading to a more accurate prediction of the resistance against the lateral failure of historic quay wall. Depending on the type of evidence, an a-priori reliability prediction for a quay wall that fails to meet safety standards can be updated to any of the three consequence classes outlined in NEN8700. In a case study, a quay wall with an a-priori reliability of $\beta = 1.5$ has been increased to $\beta = 3.2$ by including evidence of an extreme survived load of 10 kN/m^2 that resulted in displacements of less than 4 mm. This is a decrease in failure probability by two orders of magnitude, showing the potential impact of using observational information in combination with Bayesian updating.

1. Introduction

Amsterdam faces the challenge of maintaining a 200 km historic quay wall area, which is a vital part of the city's historical landscape. Many quays are currently in poor condition and require renovation or replacement in the near future, significantly impacting the city. The quay wall construction consists of a masonry cantilever wall on top of a timber floor, which is supported by headstocks situated on three to six timber pile rows. These piles are often founded on sloping canal beds. A historic technical drawing, containing the terminology of quay wall components, is presented in Figure 1. The quays are over a century old, have various configurations, and are used by road traffic, including heavy vehicles. However, signs of damage, partial collapse and warnings of such events have been observed (Korff, Hemel, and Esposito 2021). Calculating the stability and resistance of historic quay walls has shown that it is difficult to demonstrate sufficient safety. It seems that these models are too conservative, because in reality, the majority of the existing structures that proof unsafe on paper is performing quite well in practise, referring to them as "metastable". Historical quay

walls may be subjected to a variety of identified failure mechanisms, such as global stability, overturning or sliding of the masonry wall, axial bearing capacity failure of pile(s), failure of the headstocks and/or floor, lateral failure of the pile foundation, and failure of connections between headstocks and piles or sheet pile (Heming 2019). This study focuses on the lateral failure of timber pile foundations (see Figure 2). The mechanism involves soil pressure pushing the quay wall towards the canal side, countered by the lateral resistance of the pile foundation. If the active horizontal force exceeds the resistance of the pile group, lateral failure of the pile foundation can occur due to geotechnical or bending capacity failures, or a combination of them. This mechanism is considered most critical, which is supported by assessment reports as well as practical observations. Early signs of this mechanism, which are most commonly observed throughout the city centre, include leaning or bulging of the quay wall towards the waterfront, surface settlements on top and behind the quay, inclined piles, or even indications of broken piles. Furthermore this lateral failure can result in the entire quay and its foundation collapsing into the canal, having

Figure 1. Cross-section of historical quay wall structure with terminology. (Lijnbaansgracht, tussen Palmgracht en perceelno. 14, Archive of Amsterdam.)

significant consequences. Limited understanding of the lateral behaviour of historic quay walls is attributed to factors such as poor documentation of their geometry (Balestrini et al. 2021), bacterial deterioration affecting the strength of the timber piles (Pagella et al. 2021; van de Kuilen et al. 2021), and the complex interaction between closely-spaced timber piles and cohesive soils (Ashour, Pilling, and Norris 2004; Hansen and Lundgren 1960; Norris 1986). Additionally, there are uncertainties regarding the geotechnical conditions and how the active soil volume transfers its weight, the depth of the canals and the occurrence of surface loads.

This paper aims to implement Bayesian updating to reduce uncertainties in geotechnical and structural parameter distributions associated with the lateral failure mechanism of historic quay walls. Bayesian updating is a powerful method that effectively can reduce uncertainties in structural and geotechnical model input parameters, leading to a more precise understanding of the

structural safety (Beck and Au 2002; Straub and Papaioannou 2015). Information on engineering systems through monitoring, direct observations or measurements of system performances can be used to update the system reliability estimate (Straub 2011). This principle is also referred to as proven strength or reliability updating and is a well-known technique within the geotechnical and civil engineering sector (Yuen 2010).

Examples in literature are found in a variety of fields within the engineering sector. Enright et al. conducted a study focused on enhancing the prediction of future bridge conditions (Enright and Frangopol 1999). The study incorporated inspection information and engineering judgment into a quantitative assessment through the application of Bayesian updating. This was achieved using adaptive importance sampling and numerical integration methods. In the same field, Bayesian updating was used to include laboratory test data, field
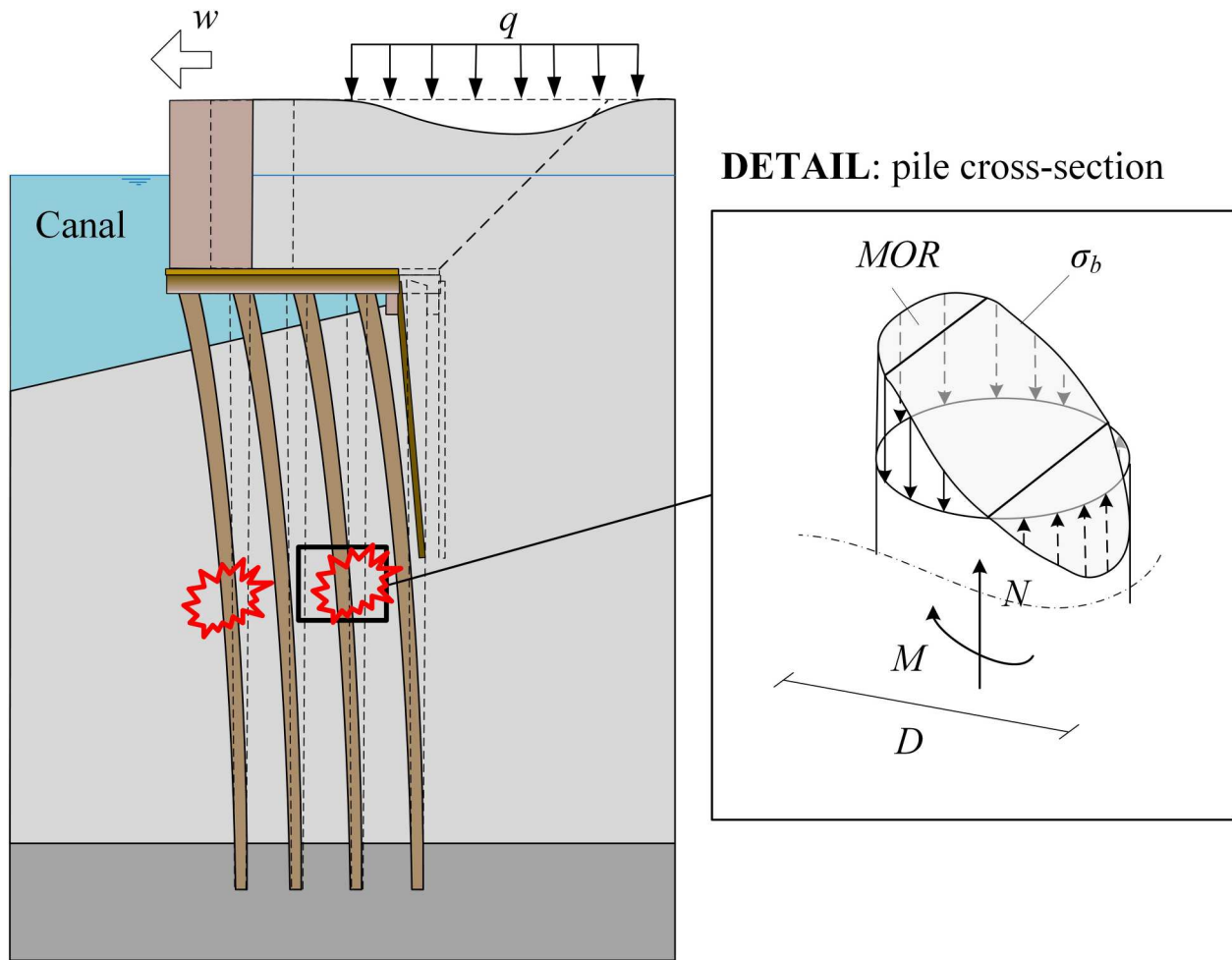
Figure 2. Failure mechanism "Lateral failure of the quay wall foundation". Detail is of pile cross-section is provided in which bending stresses are indicated.

observations and engineering judgement into the assessment of reinforced concrete bridge columns under seismic excitation (Choe, Gardoni, and Rosowsky 2007). Chung et al. applied Bayesian techniques to a simulation model of the North Edmonton Sanitary Trunk tunnel project, demonstrating significant improvement in projection accuracy (Chung, Mohamed, and AbouRizk 2006). Past performance, such as the survival of a loading condition, is an example of valuable information that can be utilised to enhance reliability estimates. Examples of such studies are survival of a phreatic level when analysing slope stability (Li et al. 2015; Zhang, Zhang, and Tang 2011) or an extreme observed water level into the assessment of the piping mechanism of dikes (Schweckendiek 2010; Schweckendiek, Vrouwenvelder, and Calle 2014). Following that same analogy, pile proof load tests are used to reduce uncertainties in the design and construction of pile foundations (Ching, Lin, and Yen 2011; Zhang 2004). Other forms of survived loading conditions during the lifetime of the structure can be traffic loads

(Gao, Duan, and Lan 2021; Yu and Cai 2019) or other service loads (such as soil retaining function or own weight).

The utilisation of Bayesian Updating in the context of quay walls is not a fully novel concept. A study conducted by Den Adel et al. (2019) explored the feasibility of incorporating performance information in the assessment of quay walls. The researchers conducted a case study involving an existing combi-wall quay structure and employed fictitious measurement data to showcase the potential impact of test loading on the reliability of the structure. To model the combi-wall quay a Blum model, which was verified using Finite Element Method (FEM), was employed. The effect of corrosion-induced degradation on the reliability of service-proven quay combi-walls was studied by Roubos et al. (2020). Including successful service conditions helped to reduce time-independent uncertainties such as the uncertainty in soil strength, leading to an increase in reliability.

The studies mentioned demonstrate that incorporating the past performance of structures or observations

into the reliability assessment can enhance the accuracy of reliability estimates and reduce uncertainties associated with individual parameters. Up to now, the application of Bayesian updating has not been explored in relation to (the lateral failure of) historic inner-city quay walls. These quays face specific challenges such as unknowns in geometric layout, complex pile-soil-pile interaction and timber degradation for which Bayesian updating can improve the assessment, thereby preventing the need for large-scale and time-sensitive replacements.

Thereto this paper presents a methodology for incorporating survival and observational information, such as the survival of extreme surface loads and observed deformations, into the reliability analysis of lateral failing historic inner-city quay walls. By integrating this information, not only does it result in a more precise and realistic estimation of failure probability, but it also allows for the reduction of uncertainties associated with individual parameters.

The lateral pile-soil-pile interaction is an essential component to include when modelling the lateral failure of quays. Soil-structure interaction is a complex and nonlinear process involving the influence of piles on the soil and vice versa, impacting neighbouring piles. Key factors influencing this pile-soil-pile interaction include pile spacing, pile diameter, pile stiffness and strength, soil properties, loading type and bed slope (Kavitha, Beena, and Narayanan 2016). Currently, computational Finite Element Method (FEM) software, such as ANSYS, ABAQUS or PLAXIS, is commonly used to solve soil-structure interaction problems accurately. However, these software models involve a significant number of mesh nodes, leading to increased computational effort (Farmaga et al. 2011; Lou et al. 2011). Bayesian updating, which requires many simulations, poses a challenge due to the demand for fast computational time (Ehre, Papaioannou, and Straub 2018). To overcome this challenge, this paper employs the analytical pile group model presented in Hemel, Korff, and Peters (2022) to simulate the lateral failure of a historic quay wall in Amsterdam. This model (briefly explained in 3.1) is computationally fast, enabling many realisations in a short period of time. With this model, forces in the pile foundation and corresponding displacements can be obtained. The model has later been validated with experiments from literature as well as field experiments and proven adequate and sufficiently accurate for calculation of limit states (Hemel 2023).

The structure and approach of this paper is as follows. First the theory of Bayesian updating and its application for inner-city quay walls is discussed in section

2. Two methods are discussed, Monte Carlo and Fragility curves. In section 3, a case study on a common type of quay wall geometry in Amsterdam is performed, demonstrating the potential of Bayesian updating. In this case study, an a-priori probability of failure is predicted for a reference period of 15 years. The probability of failure is then updated based on two types of observational evidence. The first type is evidence from an extreme survived load, while the second type involves incorporating deformation measurements taken during the extreme load event. The results of the case study are compared with NEN8700 "Veiligheidsfilosofie bestaande bouw" (Steenbergen, Vrouwenvelder, and Scholten 2012), which represents safety standards for existing buildings in the Netherlands. Section 4 discusses the approach and obtained results. Finally, conclusions are provided in section 5.

2. Bayesian updating for lateral failing historic quay walls

This section provides the theory of Bayesian updating and its application on the lateral failure of historic inner-city quay walls.

2.1. A-priori reliability analysis of lateral quay wall failure

The safety of a structure can be expressed through the resistance R of the structure, which ideally must be greater than the load S throughout its lifetime (Lin et al. 2023; Tabarroki et al. 2022). The resistance and load of a structure are typically considered as random variables, and the probability of failure P_f is the probability that the load S is greater than the strength R, as expressed in Equation (1). A more rigorous approach involves employing the "greater than or equal to" notation, as outlined by Lesny (2009); both notations are commonly utilised.

$$P_f = P[R < S] \tag{1}$$

The probability of failure can be expressed using a limit state function formulated as $Z = R - S$ (Roubos et al. 2020) in which failure of the system occurs when Z reaches a negative value. The associated failure probability is then $P_f = P[Z<0]$ and its probability of survival or reliability is defined as $P_s = 1 - P_f$. The degree of safety is often expressed by the reliability index β, which is directly related to the failure probability as per $P_f = \Phi(-\beta)$. Here, Φ is the cumulative normal distribution. For cases where the resistance and load follow simple distributions, the failure probability can be easily

solved analytically. However, in the case that the system consists of various (non-linear) components, each with its own distributions, the solution of the failure probability becomes complex. A general approach of such a complex system can be described using a continuous performance function $g(\underline{X})$ (Deng 2006). The vector $\underline{X}$ consists of a collection of random variables such as material properties, geometric properties, loads and model uncertainties. For each of these variables, an appropriate stochastic distribution must be chosen. Parameters that do not have uncertainties can be distributed deterministically. The probability of failure (or an undesired event) is given in Equation (2) (Jonkman et al. 2015). In this equation, $f_{\underline{X}}(\underline{X})$ is the common probability density function (PDF) of $\underline{X}$.

$$P_f = P(g(\underline{X}) < 0) = \int\limits_{g(\underline{X})<0} f_{\underline{X}}(\underline{X})d\underline{X} \qquad (2)$$

The system failure considered in this study is the lateral failure of the historic quay wall pile foundation, depicted in Figure 2. In this mechanism, the soil pressure at the backside of the quay wall is increased by a surface load $q[\text{kN/m}^2]$, causing a quay deflection $w[\text{m}]$ towards the canal side accompanied by the bending of the timber piles. As such, quay wall foundation piles are not only loaded axially $N[\text{kN}]$, but also laterally, introducing significant bending moments M [kNm] in the piles, which in their turn cause bending stresses σ_b [N/mm^2]. Large scale lateral 3×4 group experiments on historic quay foundation piles were performed by Hemel (2023) to study the failure of individual piles and system failure. Figure 3 illustrates the quay foundation's system failure. In Amsterdam's subsoil, timber yielding initiates at around 100 mm of group deflection, where bending stresses surpass the modulus of rupture (MOR) [N/mm^2]. Foundation piles fracture upon reaching full yielding, indicating that bending stresses exceed the MOR across the entire pile cross-section. Due to natural variation and bacterial degradation affecting pile stiffness and bending capacity, piles do not break at similar deflections. Redistribution between piles occurs, introducing redundancy to the system. Group failure is observed within the range of 200–350 mm. Notably, the transition from the onset of yielding to group failure requires only a slight additional lateral load (15%), highlighting that the onset of pile yielding should not be seen as a safe condition. The chosen failure criterion is the onset of pile yielding within the pile group. This results in the performance function $g(\underline{X},q)$ for this system in Equation (3). In here, the external diameter of the piles is indicated with $D[\text{m}]$. The corresponding a-priori probability of failure is given by

Equation (4). No serviceability limit state function is considered in this paper.

$$g(\underline{X}, q) = MOR - \sigma_b$$

$$= MOR - \left(\frac{M\theta_M}{\frac{\pi}{32}D^3} + \frac{N\theta_N}{\frac{\pi}{4}D^2} \right) \qquad (3)$$

$$P_f = P(g(\underline{X}, q) < 0) \qquad (4)$$

To describe the performance function $g(\underline{X},q)$, the analytical quay wall model is used, described in in 3.1. For the bending moment and normal force, model uncertainties θ_M and θ_N are incorporated in the limit state function, consistent with prior investigations (Roubos et al. 2020). To determine the failure probability for this particular system, several probabilistic methods are available. In this study, two methods are considered for determining the probability of failure and updating it through Bayesian techniques. These methods are Crude Monte Carlo (MC) and fragility curves (FC). The theory for estimating the a-priori probability of failure using both methods is briefly outlined.

The Monte Carlo technique is a commonly used method for determining failure probabilities in complex systems with many stochastically distributed variables (Beck and Au 2002; Jiang et al. 2015; Wang 2011). This methodology involves the use of random sampling, whereby thousands or more of calculations are performed. For each calculation, a random value is generated for each model input variable according to the corresponding chosen probability distribution. The failure probability can be determined by dividing the number of failed simulations $n_f = 1[g(X)<0]$ by the total number of simulations n ($P_{f;MC} = n_f/n$), using the *indicator function*.[1] If the sample size goes to infinity, the exact failure probability is determined. With complex computations, a Monte Carlo calculation can take a considerable amount of time or even become unfeasible.

The second method applied in this study is the use of fragility curves (Kim and Shinozuka 2004). A FC represents the conditional probability of failure P_f as function of a (dominant) loading variable s, formulated in Equation (5). Here f represents "failure" and $\underline{X}$ all random variables except for s. Fragility curves can be constructed by calculating the failure probability, in this study with FORM,[2] for a number of deterministic loads s. Between the "fragility points" linear interpolation can be used. Outside the fragility points, extrapolation can be used as long as the extrapolation takes place outside the boundaries of the area of interest.
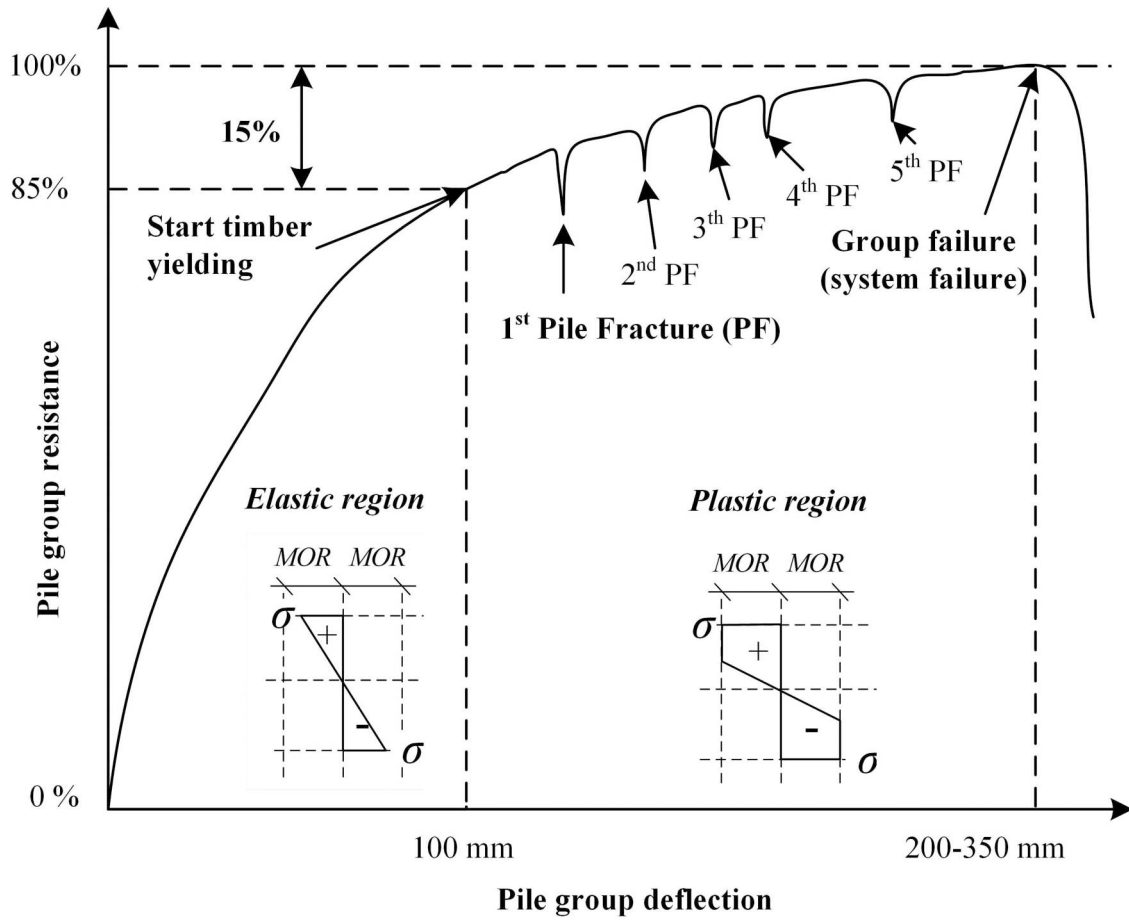
Figure 3. Failure trajectory of the quay wall system as function of the pile group deflection based on 3×4 group experiments by Hemel (2023).

An example of a fragility curve for dominant load *s* is provided in Figure 4 and indicated in black. The observation fragility curve (in red) is discussed in section 2.6
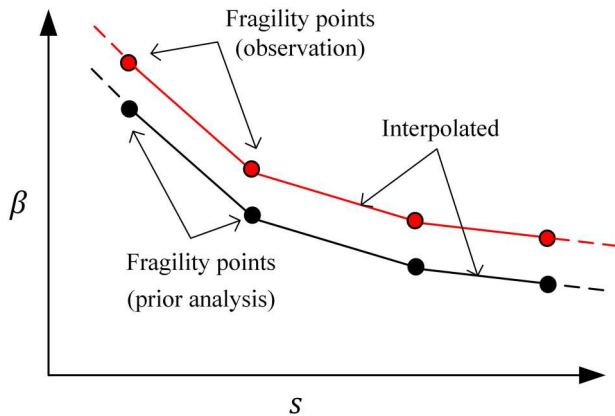
Figure 4. Example of fragility curves of dominant load *s*. In black, the FC for the reliability analysis. In red, FC including observational information in past performance.

and will be used in the posterior analysis.

$$P_{f;FC} = P(f|s) = P(g(\underline{X}, s) < 0) \qquad (5)$$

Once a fragility curve has been constructed, it is possible to determine failure probabilities for any stochastic distributed load *s* without requiring additional computationally expensive model simulations. To do so, a limit state function is used in the form $Z = s_c - s$, in which s_c is the critical load. The critical load can be determined according to Equation (6) (Schweckendiek and Kanning 2016).

$$s_c = G^{-1}(u) \qquad (6)$$

Here, *u* is the realisation of a standard normal random variable and G^{-1} is the inverse of the interpolated *β*-*s* curve $G(s) = \beta$. The problem $P_{f;FC} = P[Z<0]$ can be solved using Monte Carlo sampling.

2.2. Posterior analysis including evidence

Past performance of an existing structure is evidence *η* of its reliability and safety (Hall 1988). The simplest

example is that of a proof load. A structure survives a certain load, thus demonstrating that the resistance is at least equal to or greater than the load at the time of the proof load. This reduces the level of uncertainty associated with the resistance prior to the proof load. By taking the proof of the successful test load as evidence, the likelihood of failure will decrease and thus the reliability of the construction will increase. In addition to conducting proof load tests, there are alternative approaches to incorporate observational information into the posterior reliability analysis. For instance, one can examine successful loading conditions that the structure has endured throughout its lifespan, and integrate information derived from test data, measurements, monitoring and direct observations (Papaioannou and Straub 2012; Straub 2011). The posterior probability of failure $P_{f,p}$, given evidence η, is determined according to Bayes' rule (Bayes 1763) and presented in Equation (7). In here, the evidence η is described in terms of an arbitrary observational exceedance limit state function O, described by Equation (8).

$$
\begin{aligned}
P_{f,p} = P(f \,|\eta) &= \frac{P(f \cap \eta)}{P(\eta)} \\
&= \frac{P([g(\underline{X}) < 0] \cap [O(\underline{X}) < 0])}{P([O(\underline{X}) < 0])}
\end{aligned} \tag{7}
$$

$$
\eta \equiv O(\underline{X}) < 0 \tag{8}
$$

In the situation of multiple (k) simultaneous observations, the evidence is given by their intersection: $\eta \equiv \cap_k \{O_k(\underline{X}) < 0\}$ (Schweckendiek, Vrouwenvelder, and Calle 2014).

2.3. Evidence for historic quay walls

The posterior probability of failure for the historic quay wall system, given evidence η, is presented in Equation (9). In here, $g(\underline{X},q)$ is the performance function of the quay system. To conduct a posterior failure probability assessment, two types of evidence are considered in this study.

$$
P_{f,p} = P(f \,|\eta) = \frac{P([g(\underline{X}, q) < 0] \cap \eta)}{P(\eta)} \tag{9}
$$

The first evidence η_1 is the survival of the quay wall over its lifetime given an extreme surface load q_η [kN/m^2]. This evidence is formulated in Equation (10). Here, $\underline{X}_\eta$ is a vector of all random variables (except surface load q_η) at the time of observed survival of the quay wall. At the time of the observed extreme load, there is a positive performance function. Practical examples of extreme surface loads can be temporary storage of

cargo or heavy vehicles such as fire trucks, garbage trucks or construction equipment.

$$
\eta_1 \equiv g(\underline{X}_\eta, q_\eta) > 0 \tag{10}
$$

The second type of evidence η_2 involves expanding on the evidence presented in Equation (10) by incorporating deformation measurements. These measurements are specifically obtained at the same time as the extreme surface load was observed. Pile foundation deformations are physical coupled to timber bending stresses, which directly impact the limit state function. When large deformations occur, bending stresses are likely to be higher compared to situations with smaller deformations. If the model predictions on deformation do not align with the actual deformation measurements (i.e. if they are either too stiff or too flexible), it is a clear indication that the model input for simulating soil-structure interaction is incorrect or the model has an prediction error. Given the variation in deformation measurements along quay walls, the deformation evidence is presented as a range, including both an upper and a lower boundary. The evidence of a range of deformation measurements at the time of an extreme surface load is provided in Equation (11). Here, $W(\underline{X}_\eta, q_\eta)$ is the model predicted quay wall displacement during the observation. Furthermore, $w_{\eta,min}$[m] and $w_{\eta,max}$[m] are the lower and upper bound of the deformation measurements.

$$
\begin{aligned}
\eta_2 \equiv {}& [g(\underline{X}_\eta, q_\eta) > 0] \\
& \cap [w_{\eta,min} < W(\underline{X}_\eta, q_\eta) < w_{\eta,max}]
\end{aligned} \tag{11}
$$

2.4. Uncertainties in random variables

To calculate the posterior probability of failure of the quay system, two moments in time are considered. These are the end of the reference period for which the reliability prediction is made, and second, the moment in time when the evidence was gathered (e.g. observation of an extreme load and corresponding deformations). As stated before, a random vector $\underline{X}$ is used in the reliability prediction, while vector X_η is used at the time of evidence. Often, in the uncertainty of these vectors, a distinction can be made between epistemic uncertainty and aleatory uncertainty (Der Kiureghian and Ditlevsen 2009). Epistemic means that the modeller may have possibilities to reduce the uncertainty of the variable by collecting more information or refining the model. Aleatory uncertainties are uncertainties that cannot be reduced by collection of information. Parameters such as an

annual traffic load (other than an extreme traffic or test load) or phreatic water levels influenced by rainfall, describe a purely random process over time, and therefore are an aleatory uncertainty.

The "learning effect" in updating epistemic uncertainties is most pronounced when perfect auto-correlation in time exists. This means that parameters at the time of observation are perfectly correlated with the parameters used for the reliability prediction. Conversely, there is little to no learning effect for aleatory uncertainties. Consequently, treating an aleatory uncertainty as an epistemic uncertainty (assuming auto-correlation when there is none) may result in an underestimation of the posterior failure probability. When determining the probability of failure without utilising historical evidence data (referred to as the "prior probability of failure"), the distinction between epistemic uncertainties and aleatory uncertainties is irrelevant.

2.5. Time dependent variables

In this study, a reliability prediction for a reference period of 15 years is made, as specified by NEN8700 "Veiligheidsfilosofie bestaande bouw" (Steenbergen, Vrouwenvelder, and Scholten 2012). Because the observations are being made presently, there is a 15-year gap between the time of observation and the projected end-of-life for the quay wall. Hence, it is crucial to consider the (time-dependent) variations that may occur during this period when evaluating the reliability. Differences can be included in the random vector X at the end-of-
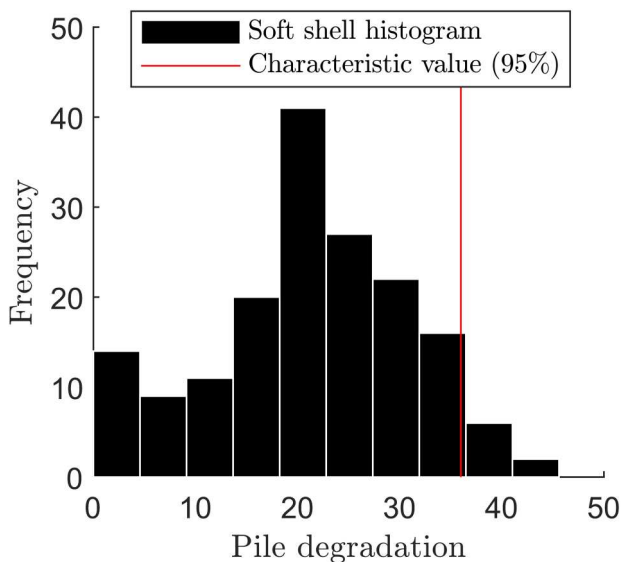
life and random vector X_η at the time of the observation, allowing for a relative "best-estimate" difference Δ (Schweckendiek et al. 2017). Three differences between the observation and the projected end-of-life are considered in this study:

- *Pile degradation:* Timber piles are subjected to bacterial deterioration (Harmsen and Nissen 1965; Varossieau 1949) influencing the strength and stiffness properties of the timber over time. The outer layers of the piles are mostly effected, creating a soft shell (without neglectable structural strength) around the core-wood (Pagella et al. 2021; van de Kuilen et al. 2021). Micro drillings were conducted on foundation piles of a quay wall that were 115 years old, located at Amsterdam Overamstel. The purpose of these drillings was to determine the thickness of the soft shell, which is illustrated in Figure 5. Based on the findings, the average thickness of the soft shell in the quay wall was determined to be 20 mm. Assuming a linear degradation of the piles over time, an effective diameter reduction of 0.34 mm/year is found. This implies that at the time of the observation, the piles are $\Delta = 5$ mm thicker compared to their expected thickness at the end of the 15-year reference period.
- *Canal bed deepening:* Deepening by bow thrusters of ships or dredging activities takes place in the canals of Amsterdam and was one of the main causes of the collapse of an Amsterdam quay wall named the "Grimburgwal" (Korff, Hemel, and Peters 2022). Lowering of the canal bed causes a reduction in lateral pile resistance and thus an increase in bending moments and bending stresses. A dredging tolerance of $\Delta = 0.2$ m is anticipated over a 15-year reference period. This projection is grounded in the operational standards of the dredgers responsible for sustaining the depth of the canals.
- *Surface load restrictions:* In the observation, 40-ton vehicles with a surface load of 10 kN/m² drove through the city centre. However, due to stricter traffic regulations, only lighter vehicles with a maximum surface load of 7 kN/m² are allowed during the remaining service life. As a result, the maximal surface load for the reliability prediction over a 15-year period is $\Delta = 3$ kN/m² lower than in the observation.

Figure 5. Pile degradation obtained with micro drilling for a population of Amsterdam quay wall timber foundation piles.

Assuming a greater strength in observation does not lead to an underestimation of the posterior failure

probability, but is rather a conservative assumption. The greater the difference between observation and the projected end-of-life, the more the posterior failure probability $P_{f,p}$ will approach the a-priori probability of failure P_f. It is important that the epistemic uncertainty in the structural and geotechnical modelling must be small (the computational model should not diverge much from reality). Otherwise, the effect of reliability updating is small and possibly unreliable.

2.6. Implementation for Bayesian updating

The posterior failure probabilities described in Equation (9) with evidence η_1 (Equation 10) and η_2 (Equation 11) is solved with Monte Carlo simulations and fragility curves. First, the sampling method Monte Carlo is evaluated. To this end, four steps are followed according to (Schweckendiek, Vrouwenvelder, and Calle 2014).

(1) **Simulation of the event to be predicted:** n realisations of each parameter from vector $\underline{X}$ are generated according to the respective probability distributions. The jth realisation of the random variable i is denoted by $\underline{X}_{ij}$. The jth realisation of the random vector is denoted by $\underline{X}_j$.
(2) **Prior probability of failure:** The prior probability of failure is determined by dividing the number of negative realisations of the performance function by n; $P_{f;MC} = \sum_j 1[g(\underline{X}_j, q) < 0]/n$.
(3) **Simulation of the event observed:** All epistemic variables maintain the same value as in simulation step 1: $\underline{X}_{\eta,ij} = \underline{X}_{ij}$ for all i where the uncertainty is to be reduced. For aleatoric variables, new realisations must be made according to their chosen distribution. For epistemic variables for which an average relative difference between observation and assessment is expected (but there is still autocorrelation in time) $\underline{X}_{\eta,ij} = \Delta + \underline{X}_{ij}$ applies, where Δ is the estimated difference between observation and assessment.
(4) **Posterior probability of failure:** The posterior probability of failure can be calculated using Equation (12), given the evidence η_1. This formula is obtained by substituting Equation (10) into Equation (9). The posterior probability of failure for the evidence η_2 is expressed in Equation (13). This formula is obtained by substituting Equation (11) into Equation (9). The evidence η_2 is incorporated in the posterior analysis by inequality updating instead of equality updating, having the advantage of postprocessing $W(\underline{X}_\eta q_\eta)$ without performing

additional computations.

$$P_{f,p;MC,\eta1}$$
$$= \frac{\sum_j \left(1[g(\underline{X}_j, q_j) < 0] \cdot 1[g(\underline{X}_{\eta,j}, q_{\eta,j}) > 0]\right)}{\sum_j \left(1[g(\underline{X}_{\eta,j}, q_{\eta,j}) > 0]\right)}$$
(12)

$$P_{f,p;MC,\eta2} =$$
$$\frac{\sum_j \left(1[g(\underline{X}_j, q_j) < 0] \cdot 1[g(\underline{X}_{\eta,j}, q_{\eta,j}) > 0] \cdot 1 \atop [w_{\eta,min} < W(X_{\eta,j}, q_{\eta,j}) < w_{\eta,max}]\right)}{\sum_j 1[g(\underline{X}_{\eta,j}, q_{\eta,j}) > 0] \cdot 1 \atop [w_{\eta,min} < W(\underline{X}_{\eta,j}, q_{\eta,j}) < w_{\eta,max}]}$$
(13)

Next, the fragility curve method is evaluated. The use of fragility curves has two major drawbacks; the first one is that deformation evidence cannot be taken into account in the assessment because the deformation is an output value that is not fully correlated with the limit state function. Second, distributions of individual random parameters cannot be refined/updated. Consequently, with the FC method, only evidence η_1 is considered. Four steps are followed according to Kanning and Schweckendiek (2017), Schweckendiek and Kanning (2016).

(1) **Fragility curve of the prediction:** Using the FORM method, the fragility curve is constructed with variable distributions from vector $\underline{X}$. For different deterministic values of q, the a-priori reliability index β is determined. Depending on the non-linearity of the β-q curve, the number of fragility points is determined.
(2) **Fragility curve of the observation:** Using the FORM method, the observation fragility curve is constructed with variable distributions from vector $\underline{X}_\eta$. For different deterministic values of q, the observation reliability index β is determined. The fragility curves for the a-priori prediction and observation are presented in Figure 4.
(3) **Critical surface load q_c:** The critical surface load is determined for the reliability prediction by $q_c = G^{-1}(u)$ and for the observation by $q_{c,\eta1} = G_\eta^{-1}(u)$. Here, G_η^{-1} is the inverse of the interpolated β-q observation curve $G_\eta(q) = \beta$ and u is the realisation of a standard normal random variable
(4) **Posterior probability of failure:** System failure due to an excessive surface load is caused by a surface load q that is greater than the critical surface load; $f = [q_c < q]$. With n realisations, the prior probability of failure can be determined using $P_{f;FC} = \sum_j 1[G^{-1}(u_j) < q_j]/n$. The posterior

probability of failure can be calculated using Equation (14), given the evidence η_1.

$$P_{f,p;FC,\eta_1} = \frac{\sum_j (1[G^{-1}(u_j) < q_j] \cdot 1[G_{\eta,j}^{-1}(u_j) > q_{\eta_1,j}])}{\sum_j (1[G_{\eta,j}^{-1}(u_j) > q_{\eta_1,j}])}$$

(14)

3. Bayesian updating for historic quay walls: a case study

In this section, a case study is performed in which the reliability of common type of quay wall geometry in Amsterdam is predicted for a reference period of 15 years and compared with reliability standards according to NEN8700. The prior probability of failure for the historic quay wall is determined using Monte Carlo and fragility curves. The prior probability of failure is then updated to a posterior probability using the Bayesian approach as discussed in 2.6. In this approach, two types of evidence are considered. The first evidence η_1 is the survival of the quay wall over its lifetime given an extreme surface load. The second type of evidence η_2 involves expanding on evidence η_1 by incorporating deformation measurements. These measurements are specifically obtained at the same time as the extreme surface load was observed. First, the quay wall model and its inputs are discussed.

3.1. Quay wall model

To describe the performance function $g(\underline{X},q)$ and displacement $W(\underline{X},q)$, an analytical quay wall model is used, depicted in Figure 6. The model consists of a framework of elastic beams embedded in an elastic foundation and is externally loaded by a soil model based on the theory of Flamant. The beam model is made up of multiple Euler-Bernoulli beams, connected to each other by boundary and interface conditions. To model the lateral bearing pile-soil-pile interactions in layered sloping soil, a method developed by Hemel, Korff, and Peters (2022) is used. The analytical quay wall model has been successfully validated through experiments found in literature, as well as experiments conducted on historical timber quay walls in Amsterdam (Hemel 2023), which makes it an accurate tool for describing failure mechanisms of quay walls with regards to lateral pile behaviour, considering both structural and geotechnical aspects.

3.2. Quay wall layout and model input

The quay wall layout used in this case study is shown in Figure 7. Within this case study, it is assumed that the quay wall has a successful past performance during its lifetime. The layout is based on common quay wall geometries in the city centre of Amsterdam, literature and previous research (Hemel 2023; Korff, Hemel, and Peters 2022; Spannenburg 2020). The quay wall consists of a gravity wall 0.8 m wide and 2.0 m high located on a floor with length 2.5 m. The floor is supported by 3 piles with diameter D, modulus of elasticity E[MPa] and modulus of rupture MOR. The piles have their toe into the first sand layer, 13.5 m below surface level. The piles have a spacing of 1 m both parallel and perpendicular to the canal. At 0.3 m behind the 3rd pile row a soil-retaining screen with a length of 4 m is present. The water level is 0.7 m below surface level, similar to the groundwater level. The fill of the quay consists of a 2 m thick sand layer, ending at floor level. Below the floor lies a peat layer with a thickness of 3 m. Below that a thick clay layer is present that goes up to the sand layer. The quay wall is loaded at a distance 2.5 m from the canal by surface load q which has a width of 2 m.

For the reliability analysis, stochastic distributions are assigned to the most dominant parameters. For the timber structure, these are the diameter, elastic modulus and MOR of the piles. For the geotechnical parameters of pile embedded layers, the most dominant ones are the cohesion c, friction angle φ, effective weight γ and stiffness k. Additionally, the friction angle and effective weight of the active soil volume behind the quay are considered dominant due to their effect on the load distribution. Table 1 shows the prior expected stochastically distributed parameters with their associated probabilities of occurrence during the remaining life. The parameters are assumed to be uncorrelated and epistemic, which is a simplification of the problem. The choice of dominant parameters is not fixed and is a choice of the designer. In this study, stochastic variables are modelled with normal distributions. While lognormal distributions are often preferred for strictly positive parameters like self-weight, cohesion, or friction angle (Kool et al. 2021), this study intentionally avoids assigning skewed uncertainties to parameters. It is emphasised that the samples drawn from the normal distribution remain positive at all times. Skewness in parameter uncertainties, if any, will be determined by the posterior parameter update, with examples provided in section 3.5.

For the model uncertainties θ_M and θ_N lognormal distributions are adapted according to the Probabilistic Model Code (JCSS 2000) for load effect calculation for moments and axial forces in frames. Quays are line-like structures, where the spatial variability of soil composition is important. This study excludes
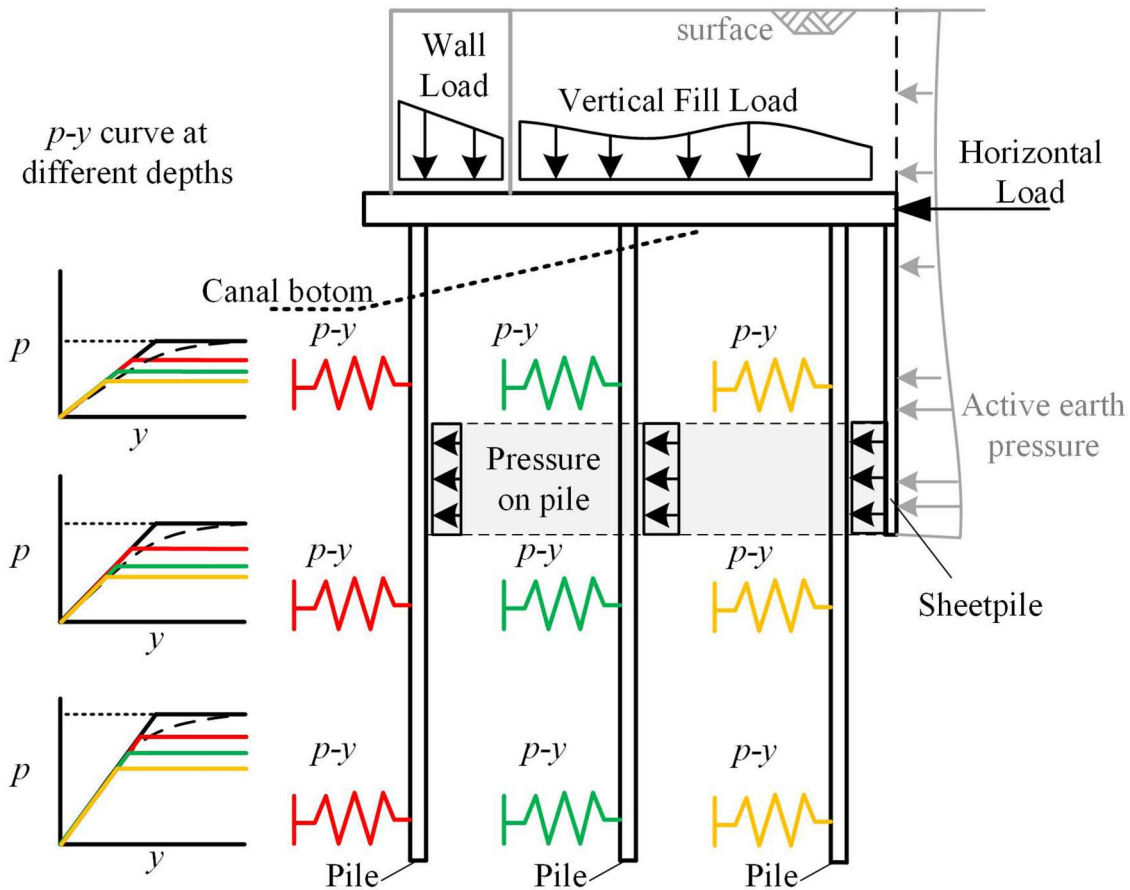
Figure 6. Schematic of analytical quay wall model in which structural members are described by beams on elastic foundations, externally loaded by an elastic soil model.

these special variations. Prior research (Choosrithong and Korff 2023) examined the spatial variability of a quay in Amsterdam, revealing variations in fill thickness and shallow peat and clay layers along a 100 m stretch. Probabilistic assessments of dikes in the Netherlands (Kool et al. 2021; Pol et al. 2021) incorporated spatial variations, offering a methodology applicable to quay walls.

The reliability prediction is performed for a surface load of $q = 7$ kN/m^2. This is the maximal allowed traffic load that is permitted in the remaining service life of the quay, based on a 15 ton truck. This case study thus assumes that over the next 15 years, there will be a regular occurrence of critical loads of 7 kN/m^2 with certainty. The surface load q is stochastically distributed with a coefficient of variation (CV) of 0.2 since there is an uncertainty in the force distribution from the truck wheels towards the soil. This distribution uncertainty is autocorrelated in time. For instance, if the surface load at the observation is 10% larger than the mean, it can be expected that the surface load will also be 10% larger than the mean at the end-of-life period. At the observation (now), the diameter is measured 0.245 m on average and expected

to degrade to 0.24 m at the end of the 15-year reference period. The diameter has a CV = 0.1 based on field experiments, dive reports and data studies. The *MOR* is taken 22 N/mm^2 with CV = 0.1 and the modulus of elasticity is taken 9000 MPa with CV = 0.2. The (NEN-EN9997-1 2012) is used to estimate the variation coefficients of the geotechnical parameters. Cohesive soil layers are modelled as drained due to the long time scale.

3.3. Prior probability of failure

The prior probability of failure is made for a 15 year service life time. As such, a degraded pile diameter of 0.24 m, a canal bed deepening of 0.2 m and a 7 kN/m^2 surface load are used in the prediction. A summary of the prior probability of failure analysis for the Monte Carlo and Fragility curves methods is given in Table 2. The probability of failure after 15 years service life, obtained with MC is $P_{f;MC} = 6.65 \cdot 10^{-2}$ and with FC is $P_{f;FC} = 6.02 \cdot 10^{-2}$. The joint probability density function of the quay wall system is presented in Figure 8, which includes both failing and surviving samples from the Monte Carlo simulations. The sensitivity factors,
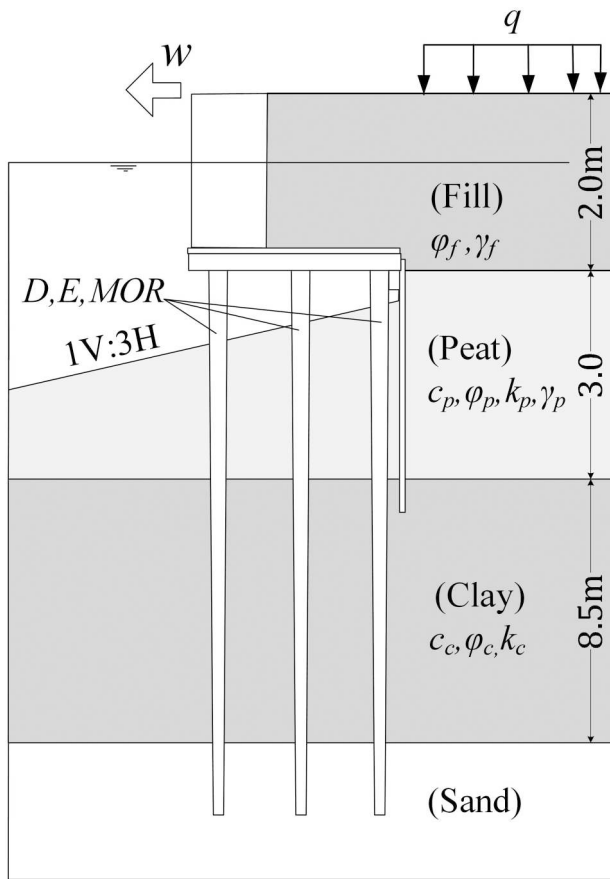
Figure 7. Schematic cross section of quay wall layout. Stochastic variables are indicated. Lateral deflection of the quay is described by w.

obtained with FORM are presented in Figure 9. It can be seen that the uncertainty in the pile diameter has the biggest impact on the system reliability with a sensitivity factor of $\alpha^2 = 0.668$. The pile diameter significantly impacts bending stress (power-3), pile flexural rigidity (power-4) and ultimate bearing soil pressure, creating an exponential dependency on the limit state function.

Table 1. Stochastic distributed input parameters and their distributions.

Variable	Unit	Type	Mean	CoV
q	kN/m^2	Normal	7	0.2
D	Mm	Normal	240	0.1
MOR	N/mm^2	Normal	22	0.1
E	MPa	Normal	9000	0.2
φ_p	deg.	Normal	15	0.1
c_p	kN/m^2	Normal	6	0.2
φ_f	deg.	Normal	30	0.1
φ_c	deg.	Normal	28	0.1
c_c	kN/m^2	Normal	4	0.2
k_p	kN/m^3	Normal	10,00^{3}0	0.2
k_c	kN/m^3	Normal	4300	0.2
γ_v	kN/m^3	Normal	2	0.05
γ_z	kN/m^3	Normal	8(sat)18(dry)	0.05
θ_M	–	Lognormal	1	0.1
θ_N	–	Lognormal	1	0.05

Table 2. Prior probability of failures for historic quay wall example.

Method	P_f	β	Samples	Simulation time (single pc)
MC	$6.65 \cdot 10^{-2}$	1.51	10,000	∼ 3.5 d
FC	$6.02 \cdot 10^{-2}$	1.54	318	∼ 4.8 h

Meanwhile, the system's resistance (*MOR*) lacks this exponential factor, resulting in a much smaller influence factor. Other dominant parameters ($\alpha^2 > 0.04$), are the cohesion of the peat c_p ($\alpha^2 = 0.125$), the surface load q ($\alpha^2 = 0.067$), effective weight of the fill γ ($\alpha^2 = 0.048$) and the friction angle of the peat φ_p ($\alpha^2 = 0.041$).

For the Monte Carlo simulations, 10,000 samples were used for both the prior and posterior calculations. In Figure 10, it is substantiated that with the chosen sample size, the model converges strongly towards the FC outcomes for both prior and posterior simulations, indicating a stable and accurate model prediction. For the FC approach, 6 fragility points are computed with the FORM method, requiring only 5% of the number of MC simulations. Another advantage of FC compared to MC simulations is the ability to calculate the prior probability of failure for any stochastic distribution of the surface load q after constructing the fragility curve, without requiring additional computationally expensive model simulations.

Based on NEN8700, the Dutch regulations for existing structures, three consequence classes are applicable to structures with a reference period of 15 years: CC3, CC2 and CC1b. These consequence classes correspond to reliability indexes of 3.3, 2.5 and 1.8 respectively. However, with a predicted reliability of approximately 1.5, the quay wall in this case study does not meet any of the requirements for the three consequence classes. Consequently, this quay wall fails to meet the necessary safety requirements.

3.4. Posterior probability of failure – extreme load survival

In this section, the prior probability of failure is updated with evidence η_1, which is the survival of the quay wall over its lifetime given an extreme surface load q_η. Between the moment of observation and the time for which the reliability prediction is made, changes to the quay wall have taken place. As discussed in section 2.5, three time effects are taken into account. Firstly, the pile diameter at the observation is 0.245 m, which degrades to 0.24 m at the end-of-life period. Secondly, the canal bed is 0.2 m higher at the observation than at the end of the 15 year reference period as a consequence of bow thrusters and dredging maintenance. Lastly, for the reliability prediction, the surface load is taken as q
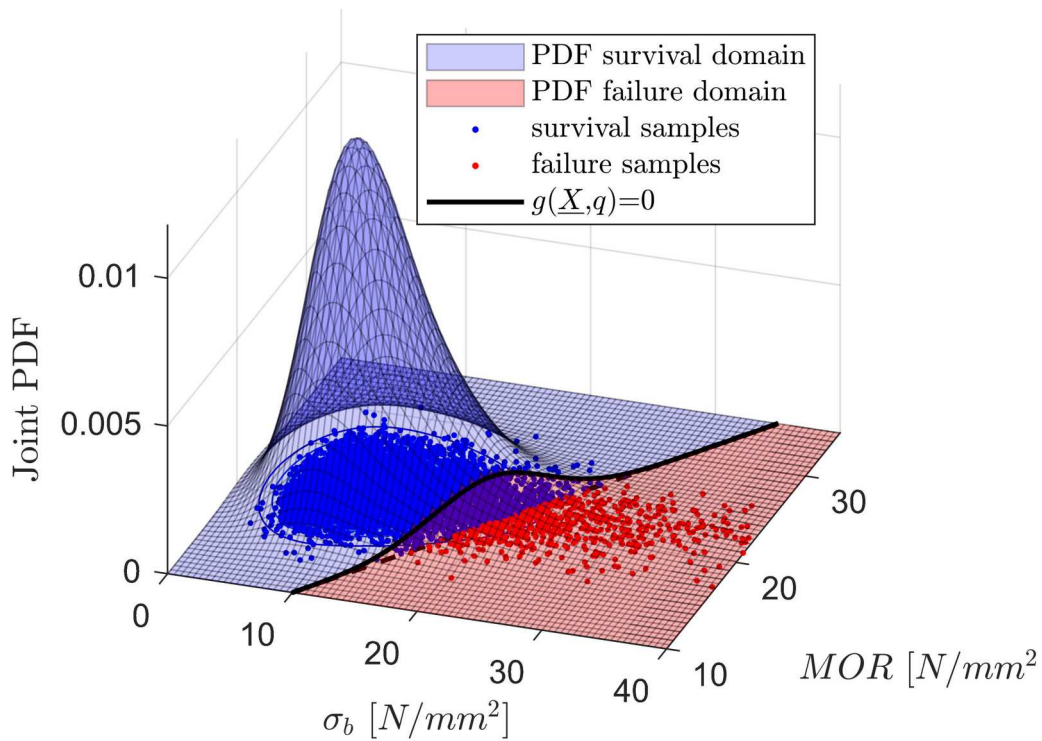
Figure 8. Joint PDF of quay wall system indicating the failure and survival domain.
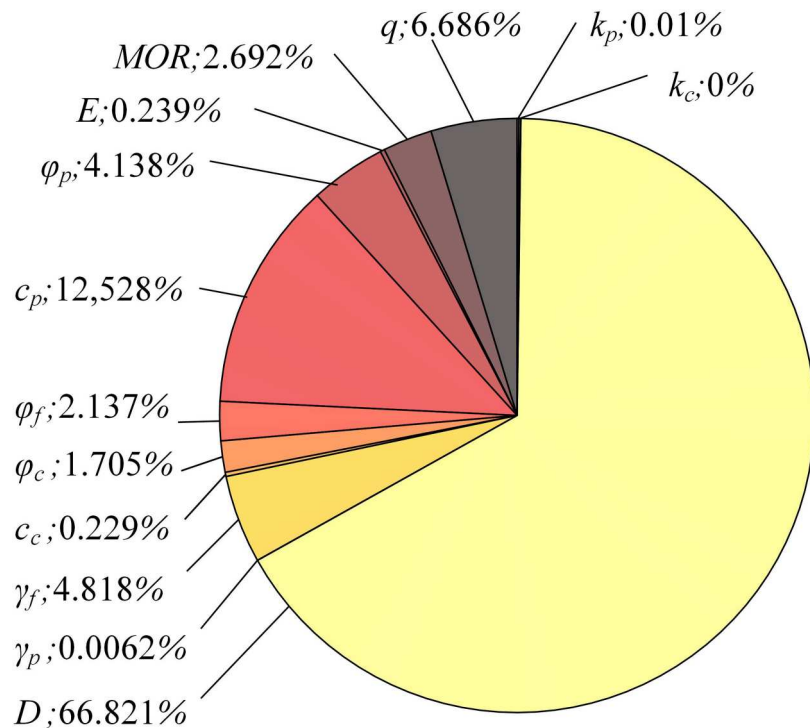

Figure 9. Sensitivity factors α^2 obtained with FORM computation.

$= 7$ kN/m², while during the observation, the surface load is $q_\eta = 10$ kN/m². A summary of the posterior probabilities of failure analysis for the Monte Carlo and Fragility curves methods is given in Table 3. For reference,

the prior probabilities of failure are also provided. The probability of failure is reduced by a factor 3.

First, the effect of Bayesian updating is demonstrated by the Monte Carlo sampling method. In Figure 11,
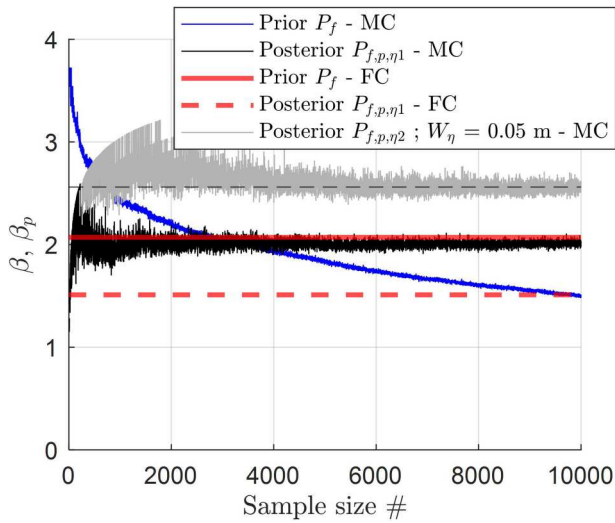
Figure 10. Reliability for a-priori and posterior MC realisation as function of the sample size compared with FC realisation.

Figure 12. Posterior Monte Carlo sampling of reliability prediction.

Table 3. Prior and posterior probabilities of failure; given evidence η1.

Method	P_f	β	$P_{f,p;\eta 1}$	$\beta_{p;\eta 1}$
MC	$6.65 \cdot 10^{-2}$	1.51	$2.31 \cdot 10^{-2}$	1.99
FC	$6.02 \cdot 10^{-2}$	1.54	$1.96 \cdot 10^{-2}$	2.06

sampling calculations have been made using random vector $\underline{X}_\eta$ and q_η as model inputs. It is not possible to have the realisations (in grey) where the performance function $g(\underline{X}_\eta, q_\eta)$ is negative, as there is evidence that the quay wall has not failed in the observation. The dark blue and light blue dots are the remaining realisations where the quay wall does not fail. The remaining
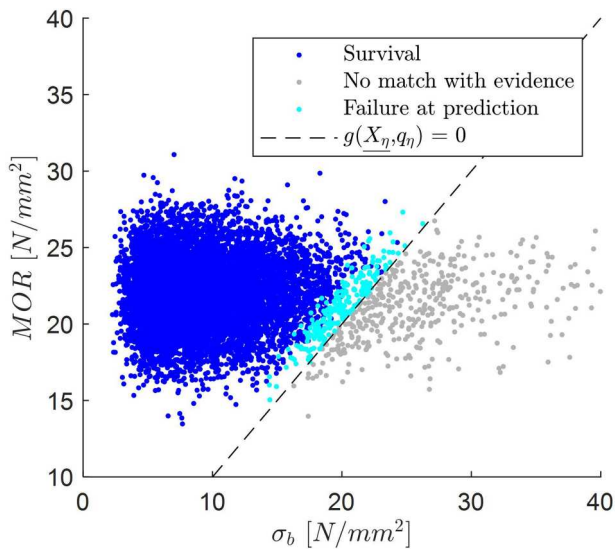
realisations $g(\underline{X}_\eta, q_\eta) > 0$ are used in the reliability prediction which is shown in Figure 12. In this figure, the blue dots are the survival realisations while the red dots are the failing realisations. The light blue points in Figure 11 indicate realisations that survive in the observation but fail in the reliability prediction. Light blue realisations in the observation fail in the prediction due to time-related effects considered, which weaken the quay wall over time. The decrease in pile diameter increases bending moments and reduces the moment of inertia, leading to higher bending stresses in the timber piles. Additionally, the canal bed deepening reduces
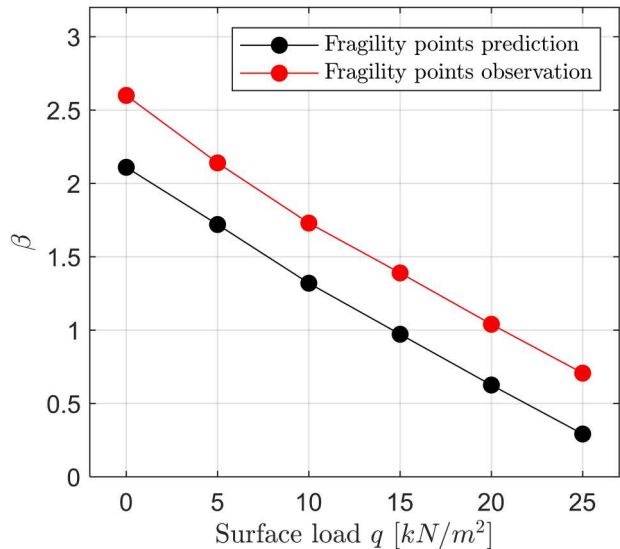

Figure 11. Monte Carlo sampling of observation with extreme surface load evidence.

Figure 13. Fragility curves obtained with FORM. Fragility curve at observation in black and at prediction in red.
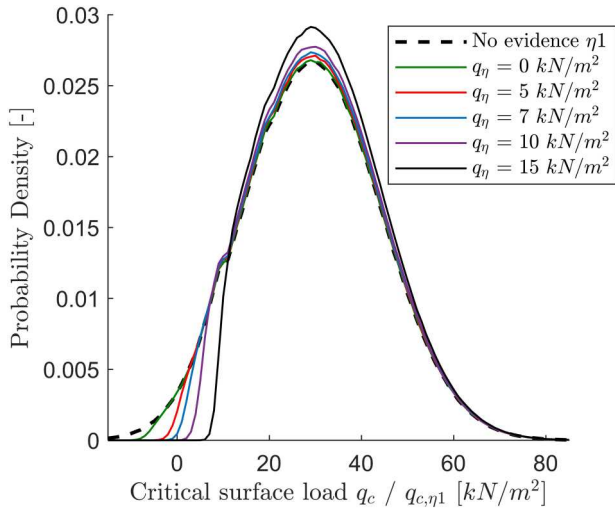
Figure 14. Critical surface load PDF. Dashed line represents prior analysis without evidence. Coloured lines represent critical surface loads with surface loads evidence.

lateral support, further increasing bending moments and stresses in the timber.

Second, the effect of Bayesian updating is demonstrated using the fragility curve method. The fragility curves for the prediction and observation are presented in Figure 13. The fragility curve for the observation has on average a higher reliability which is due to the elevated canal bed and a larger pile diameter. Figure 14 displays multiple critical surface loads. The critical surface load for the a-priori prediction, denoted as q_c, represents the scenario without any evidence at the end of the service life time. On the other hand, the critical surface loads at the moment of an observed extreme surface load, q_η, is denoted as $q_{c,\eta1}$. Both q_c and $q_{c,\eta1}$ are utilised in Equation 14 to calculate the posterior probability of failure, $P_{f,p;FC,\eta1}$. The resulting posterior probabilities of failure are presented in Table 4. It is observed that with larger extreme loads observed in the past, the left tail of the critical surface load $q_{c,\eta1}$ at the time of observation shifts to the right, ultimately increasing the reliability of the structure in the prediction for a reference period of 15 years. Even without an observed surface load ($q_\eta = 0$ kN/m²), the reliability of the structure increases. This is because the pile foundation of the quay is laterally loaded by the active earth pressure behind the quay, even in the absence of any surface load. Quay walls can fail without the presence of top loads, as observed in the case of Grimburgwal

(Korff, Hemel, and Esposito 2021). Therefore, evidence of "survival" without any observed top load is already valuable.

3.5. Posterior probability of failure – extreme load survival with deformation measurements

In this section, the prior probability of failure is updated using evidence η_2. This evidence pertains to the quay's successful past performance given an extreme observed surface load of 10 kN/m², while simultaneously considering the availability of quay wall deformation measurements taken at the same time of the observation. The deformation measurements, which capture a range of displacements along the quay wall and span the interval $[w_{\eta,min}, w_{\eta,max}]$. In this case study, it is assumed that all displacements of the quay wall are caused solely by the deflection of the pile foundation below the quay. Deformations resulting from, for instance, the sliding of the gravity wall or the tilting of the gravity wall are not considered. Time effects between observation and prediction are included as discussed in section 2.5.

The interval $[w_{\eta,min} = 0.02$ m, $w_{\eta,max} = 0.08$ m] is considered at the time of the observation. The Monte Carlo sampling at observation is presented in Figure 15. The horizontal axis contains the performance function $g(\underline{X}_\eta, q_\eta)$, shown in Equation (3), and the vertical axis the displacement $W(\underline{X}_\eta, q_\eta)$. The relationship between displacement and the performance function shows a negative correlation, as larger deflections are associated with higher bending stresses. Consequently, quay walls with greater deflections are considered weaker. However, it's important to note that displacements and deflections are not fully correlated to the bending stresses. This lack of full correlation is the reason why the FC method cannot incorporate deformation evidence. The grey realisations in Figure 15 represent realisations where the performance function is negative (indicating failure) and the displacement observation function is not fulfilled. The dark blue and light blue dots are the remaining realisations where the quay wall does not fail and deflects within the range of measured deflections. The remaining realisations are used in the prediction which is shown in Figure 16. In this figure, the blue dots are the survival realisations while the red dots are the failing realisations. Observing the "survived realisations" (in Figure 15)

Table 4. Posterior probability of failures for multiple observed extreme load survivals obtained with fragility curve method.

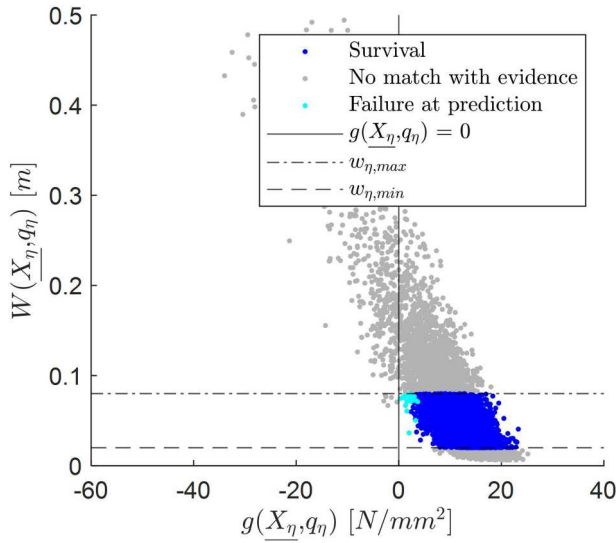| q_η [kN/m²]	0	5	7	10	15	Prediction (no evidence η1)
$P_{f,p;FC,\eta1}$ [–]	5.56·10⁻²	4.54·10⁻²	3.73·10⁻²	1.96·10⁻²	0	$P_{f;FC} = 6.02·10⁻²$
$\beta_{p;FC,\eta1}$ [–]	1.58	1.69	1.78	2.06	∞	$\beta_{FC} = 1.54$

Figure 15. Monte Carlo sampling of observation with extreme surface load evidence in combination with deformation measurements.

Figure 17. Posterior reliability index as function of displacement evidence for $q = 7$ kN/m^2 and $q_\eta = 10$ kN/m^2.

represented by the light blue and blue dots, it becomes apparent that the deflection and bending stress values increase when utilised in the prediction (in Figure 16). This increase is a result of the time effects that take place over the remaining lifespan of the quay wall, ultimately leading to failure for certain realisations. The posterior probability is updated according to Equation (14) from $P_{f;MC} = 6.65 \cdot 10^{-2}$ to $P_{f,p;MC,\eta2} = 4.20 \cdot 10^{-3}$ which is an increase in reliability from $\beta_{MC} = 1.51$ to $\beta_{p;MC,\eta2} = 2.63$.

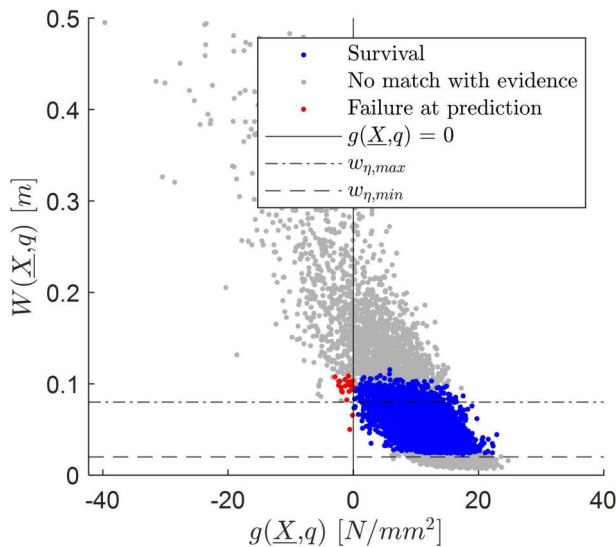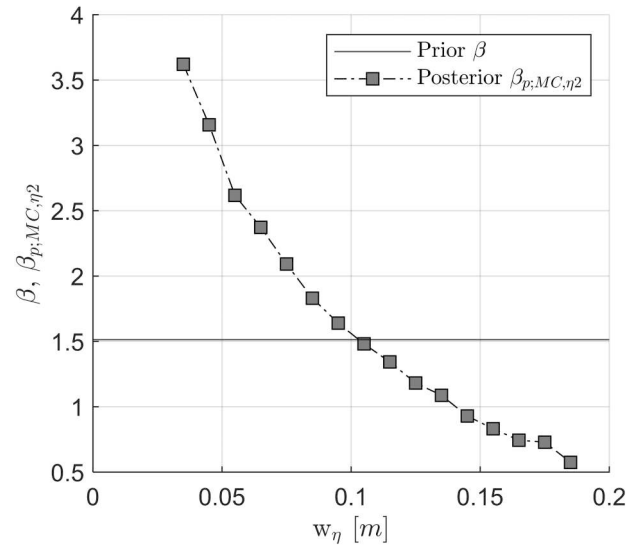Observations do not necessarily lead to a reduction of the a-priori probability of failure. To demonstrate

the effect of observed deformations on the posterior failure probability, the reliability index was set against the observed mean deformation w_η[m], depicted in Figure 17. The mean deformation is defined by $w_\eta = (w_{\eta,min} + w_{\eta,max})/2$. The difference between $w_{\eta,min}$ and $w_{\eta,max}$ is kept constant with 0.06 m. For comparison, the a-priori reliability index is plotted. It can be seen that an increase in observed deformations results in a decrease of the reliability of the quay wall. With 0.1 m of displacement, the posterior reliability becomes smaller than the prior reliability. The maximal reliability which can be obtained with 10^4 samples is $\Phi^{-1}(10^{-4}) = 3.72$, resulting in no reliability estimate for deflections

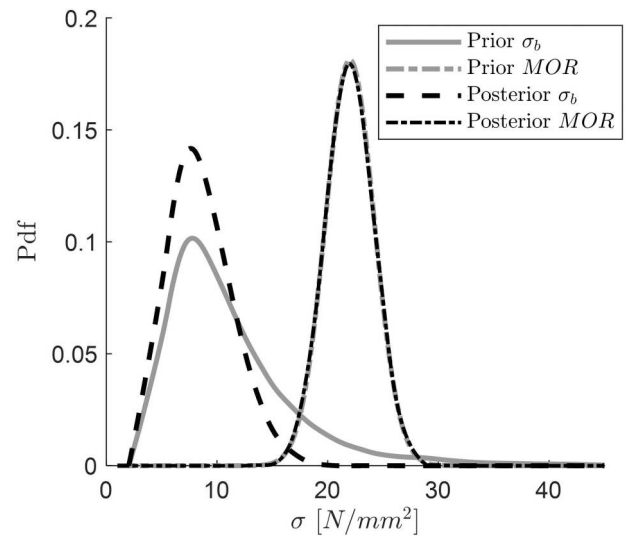**Figure 16.** Posterior Monte Carlo sampling of reliability prediction.

Figure 18. Prior and posterior *MOR* and σ_b. For $w_{\eta,min} = 0.00$ m and $w_{\eta,max} = 0.06$ m. Surface loads are $q = 7$ kN/m^2 and $q_\eta = 10$ kN/m^2.
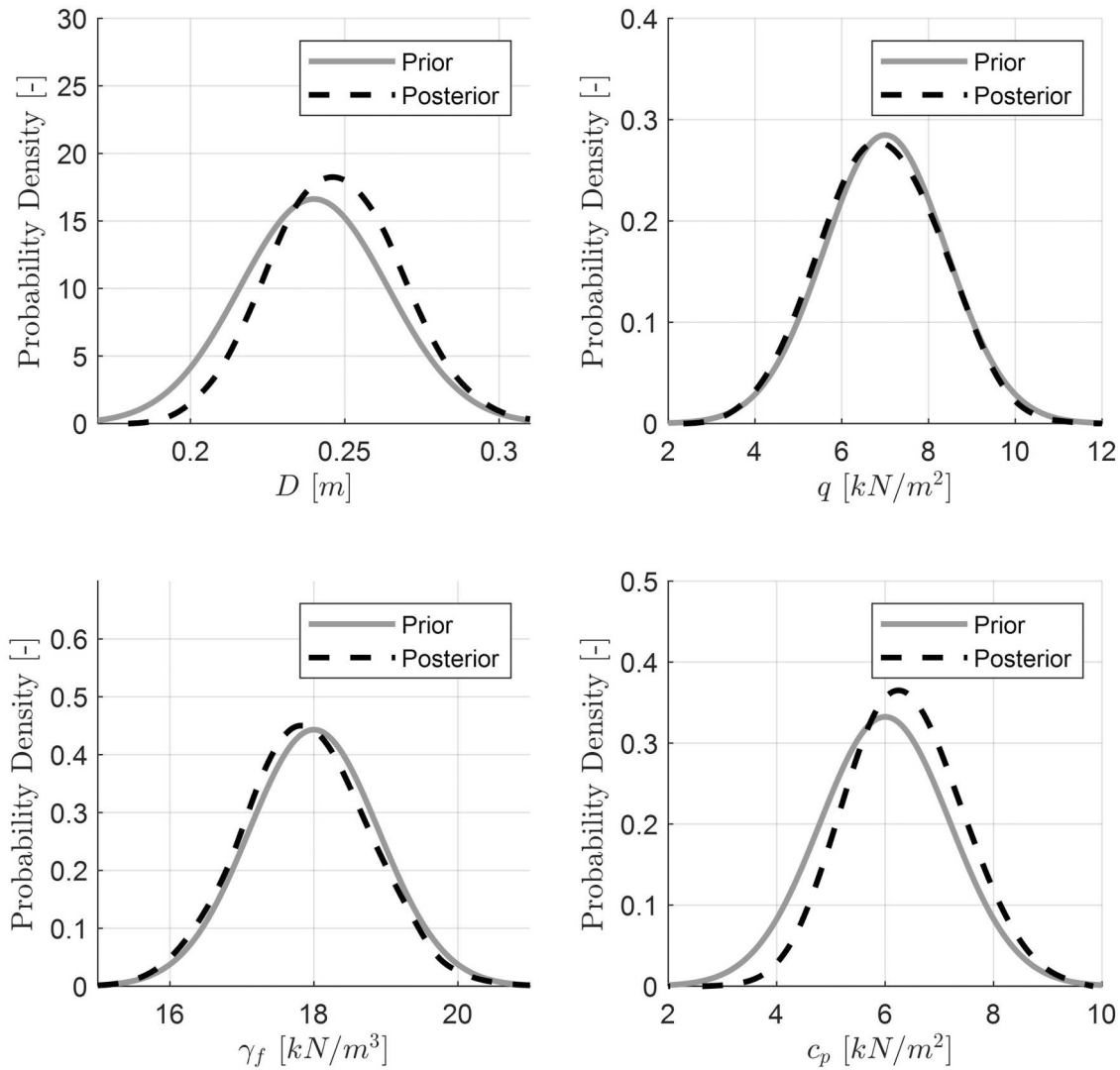
Figure 19. Prior and posterior stochastic distributions of individual parameters – evidence $w_{\eta,min} = 0.00$ m and $w_{\eta,max} = 0.06$ m. Surface loads are $q = 7$ kN/m² and $q_\eta = 10$ kN/m². Top left is the diameter D, top right is the surface load q, bottom left is soil weight of the sand fill and bottom right is the cohesion of the peat layer c_p.

smaller than 0.03 m. Note the β-w plot in Figure 17 is influenced by surface load q and also by the observed surface load q_η.

A more general way to present the updated system is in terms of modulus of rupture (*MOR*) and model computed bending stresses (σ_b) which are the two main parameters in the performance function. For displacement range [$w_{\eta,min} = 0.00$ m, $w_{\eta,max} = 0.06$ m], the prior *MOR* and σ_b are visualised in Figure 18. It can be seen that Bayesian updating for quay walls primarily updates the model computed bending stress of the system, as 97% of the influence factors affect this parameter. The modulus of rupture of piles is hardly updated, as its influence factor is less than 3%. The posterior estimation shows a considerable reduction in the right tail of the bending stress compared to the prior

estimation. This reduction leads to higher posterior system reliability. Figure 19 shows the impact of Bayesian updating for the most dominant parameters, namely the pile diameter D, cohesion of the peat c_p, the surface load q as well as the effective weight of the fill γ for displacement range [$w_{\eta,min} = 0.00$ m, $w_{\eta,max} = 0.06$ m]. Parameter updating has the most significant impact the diameter and cohesion of the peat layer (together 80% of the influence factors). When evidenced deformations are small, the pile diameter tends to shift towards larger values, and the cohesion, which provides support pressure to the piles, shifts towards higher values during the postdiction. The reduction of the right tail in the a-priori computed bending stress shown in Figure 18 is primarily attributable to the updating of the pile diameter and the cohesion of the peat layer.

Table 5. Summary on prior and posterior reliability index for various observations.

Method	Observation evidence	Prior β	Posterior β_p^-
MC	$q_\eta = 10$ kN/m^2	1.51	1.99
MC	$q_\eta = 10$ kN/m^2 & 0 m $<w_\eta<$ 0.04 m	1.51	>3.72–3.2
MC	$q_\eta = 10$ kN/m^2 & 0.04 m $<w_\eta<$ 0.10 m	1.51	3.2–1.47
MC	$q_\eta = 10$ kN/m^2 & 0.10 m $<w_\eta<$ 0.20 m	1.51	1.47–0.44
FC	$q_\eta = 0$ kN/m^2	1.54	1.58
FC	$q_\eta = 5$ kN/m^2	1.54	1.69
FC	$q_\eta = 7$ kN/m^2	1.54	1.78
FC	$q_\eta = 10$ kN/m^2	1.54	2.06
FC	$q_\eta = 15$ kN/m^2	1.54	∞

3.6. Interpretation of case studies

Observations from the past can have a significant impact on the posterior reliability of historic quay walls. A summary of the various simulations and methods can be found in Table 5. Evidence of extreme observed surface loads during a test load (e.g. $q << q_\eta$) without failing, can increase the reliability of quay walls by multiple orders of magnitude. The same is true for deformation evidence, in which the reliability index can increase to over 3.7 in case of small deflections observed in the past (e.g. <0.04 m). However, evidence of large deformations (e.g. >0.1 m) can be proof that a quay wall has a high risk to fail. The case study presented in this paper was conducted for a reference period of 15 years. To interpret the values listed in Table 5, the guidelines specified in NEN8700, known as "Veiligheidsfilosofie bestaande bouw" in Dutch, are employed. For structures with a reference period of 15 years, three consequence classes are defined: CC3, CC2 and CC1b, each corresponding to specific reliability indexes of 3.3, 2.5 and 1.8, respectively. The case studies indicate that, depending on the evidence, the posterior reliability can fall within any of the 3 consequence classes, if the a-priori prediction suggests insufficient safety.

4. Discussion

First, the limitations of the used quay wall model, and its effect on the results are discussed. The applied analytical quay wall model does not take into account loading history. Repetitive loadings from the past causes (plastic) deformations in the long term. Combined with time effects such as soil creep and timber relaxation, model deformations but also bending stresses may be inaccurate, but are believed to be conservative. Furthermore, the modulus of rupture and the modules of elasticity of the timber are time- and load dependent (van de Kuilen et al. 2021). This effect is not included, possibly overestimating the posterior reliability. The dependence of timber strength on its loading history is one of the greatest challenges for the intended application. This aspect should be further considered by timber experts. To take into account these kinds of effects, more complex software is needed. However, increasing the complexity of models results in greater computational times, making sampling methods less attractive. It is necessary to find a balance between the computational complexity and the computational speed. To overcome this challenge, it is advised to perform deterministic time-dependent computations using FEM software. These computations should include the effects mentioned earlier and assess their impact on the overall force distribution within the foundation. By calibrating the analytical model based on these computations, it can still be used in the probabilistic Bayesian analysis conducted in this paper. If the use of FEM models is still desired, it is advised to employ the fragility curve approach as it significantly reduces computational effort (more than 18 times in this study) compared to Monte Carlo simulations.

Second, a discussion on Bayesian updating on lateral failing quay walls is provided. In this analysis a simplification has been made; the maximum deformation of the quay wall is only due to the greatest load the quay has experienced during its lifetime. Furthermore, extreme events from the past may have weakened the quay wall structure. As a result, there will no longer be a perfect correlation between the moment of observation and the prediction. Moreover, assuming stochastic parameters to be uncorrelated may lead to an overestimation of the system's reliability. For instance, the modulus of rupture and modulus of elasticity are strongly correlated (Pagella et al. 2022). Other examples of correlations between stochastically distributed parameters include the densities of soils and friction angles, as well as the stiffness of the soil and cohesion and friction angle.

Third, a discussion on the applied probabilistic methods is given. In the Monte Carlo analysis, 10,000 samples were used to demonstrate the potential of reliability updating, which is a bit low. For further analysis, it is advised to perform more computations in order to get a higher accuracy. Promising methods to drastically reduce computational time are importance sampling or surrogate modelling which is roughly similar to the computational time needed for FORM.

Lastly, the practical implementation and applicability of Bayesian updating for quay walls in the city centre of Amsterdam are discussed. The quay configuration, as well as the soil and structural parameters used in this study, are highly representative of the quay walls found in the city centre of Amsterdam. Notably, examples such as Grimburgwal and Herengracht

(Spannenburg 2020) feature quay walls with three piles, although the exact length in metres this type of quay is not known. However, Amsterdam has many quay walls which all have a unique configuration. Variation in the number of piles, the retaining height, the location of the soil retaining screen, the presence of trees and the traffic intensity may be present. Therefore, it cannot be said in advance whether the impact of proven strength will be similar to other quay wall configurations. Further exploratory studies should be undertaken to demonstrate the impact of Bayesian updating on different configurations of quay walls, utilising similar observations. Furthermore, only two types of evidence are included in the posterior assessment of lateral failing quays. However, evidence can be collected through various monitoring methods, such as measuring pile rotations, surface settlements, or lateral soil deflections behind the quay.

A more general aspect to consider is that the method in this study includes only one failure mechanism. The failure of a quay wall is usually a combination of different failure mechanisms, as the study of the collapsed Grimburgwal (Korff, Hemel, and Esposito 2021) showed. By taking into account multiple failure mechanisms in the analysis, it can be better clarified what the impact of proven strength is on the posterior reliability. It is important to note that different failure mechanisms may require different types of evidence. For instance, to assess the overturning of the masonry wall, deflection and rotation measurements can be utilised. Similarly, settlement data from the masonry wall or the piles themselves can be used to evaluate the vertical settlement of the entire pile foundation.

5. Conclusion

This paper describes how evidence of survived loading situations and related deformations that occurred in the past can be quantitatively taken into account in the reliability assessment of historical quay walls. The application of the available theory to a quay wall on laterally loaded piles is, as far as is known, done for the first time and the results show that this is feasible and has a lot of potential. Two methods, Monte Carlo sampling and fragility curves, were used to implement the theory of proven strength. With MC individual parameters, individual parameters such as pile diameter and cohesion of soils can be updated, which is not possible with fragility curves. However, the MC method is computationally expensive compared to the fragility curve method. Once a fragility curve has been constructed, it is possible to determine failure probabilities for any

stochastic distributed load without requiring additional computationally expensive model simulations.

A case study on a quay wall was performed, demonstrating the potential of Bayesian updating. In this case study, an a-priori probability of failure was predicted for a reference period of 15 years. Subsequently, the probability of failure was updated by considering two types of observational evidence. The first type involved evidence derived from an extreme survived load, while the second type incorporated deformation measurements obtained during the extreme load event. Based on the findings, the following conclusions can be drawn:

- Depending on the evidence, the posterior reliability can fall within any of the three consequence classes (CC3, CC2 and CC1b outlined in NEN8700), if the a-priori prediction suggests insufficient safety and strength. Updating can thus have a significant effect on the reliability estimate.
- The greater the observed extreme surface load compared to the surface load used in the prediction, the greater the difference between prior and posterior reliability of the quay wall.
- If there is a large difference between the structural condition of the quay wall at the time of observation and the time of the reliability prediction, the effect of the observations on the posterior reliability decreases. Large differences between observation and prediction can be caused by, for example, pile degradation, deepening of the canal or a reduction of the timber strength due to time effects.
- Deformation measurements at the time of observation have a strong influence on the updating of a prior determined failure probability. Small deformations lead to a small failure probability while large deformations lead to a large failure probability. The deformation of the pile foundation is strongly correlated with the bending stresses within the foundation itself. It is anticipated that larger deformations correspond to higher bending stresses, and vice versa.
- Bayesian updating has the greatest impact on parameters with high influence factors. In the case study, the pile diameter and the cohesion of the shallow peat layer showed the largest differences between prior and posterior parameter uncertainties.

The following recommendations are given:

- In order to test the applicability and robustness of Bayesian updating on quay walls, it is important to consider different case studies. Variations can be

made in the main characteristics of the quay wall for each case.

- Further research is needed in methods to include the load history of quay walls. Repetitive loading, soil- and timber creep, and strength reduction over time are effects that are of paramount importance to be included in the reliability prediction of historical quay walls.
- By performing non-destructive tests in the city centre (operational load testing), additional evidence can be obtained about quay walls. For example, a truck can be parked as a static load for a certain period of time on a quay wall while the deformations are measured at the same time. This methodology must be carefully studied to determine the extent to which the load test has caused permanent damage to the quay wall. In the case of a load test, it is necessary to make an esti- mation in advance of the probability of damage/fail- ure and corresponding deformations, both of which should be sufficiently low.
- To make more reliable failure probability analyses, it is important to conduct further research into the cor- relation between randomly distributed parameters.
- Uncertainties concerning parameters can be reduced by conducting on-site inspections and investigations. It has been revealed that pile diameter is the most dominant parameter. By conducting further research into the pile diameter at the location to be assessed, a large part of the uncertainty can be eliminated.
- It is recommended to systematically apply the method to any structures whose exact geometry and loading history are known. Ideally, a simple model similar to the one used in this study should be used, but calibrated with finite element models and/or with a loading test.
- The principle of Bayesian updating can significantly influence the failure probability related to various failure mechanisms in quay walls. It is recommended to explore the potential of Bayesian updating for assessing other failure mechanisms as well.

Notes

1. The indicator function is represented by 1[]. This means that if the criterion inside the brackets is met, the output of 1[] is equal to 1; if not, it is equal to 0.
2. FORM (First Order Reliability Method) is seen as a good alternative to the "brute force" Monte Carlo method (Bai 2003). The method is an accurate approxi- mation that requires significantly fewer calculations to determine the failure probability. FORM approximates the failure probability by linearising the performance function $g(\underline{X})$ with the help of Taylor series at the design point. With the FORM method, the sensitivity factor a_i can be determined for each variable.
3. In the PDF, this value is not centered well

Disclosure statement

No potential conflict of interest was reported by the author(s).

References

Ashour, M., P. Pilling, and G. Norris. 2004. "Lateral Behavior of Pile Groups in Layered Soils." *Journal of Geotechnical and Geoenvironmental Engineering* 130 (6): 580–592. https://doi.org/10.1061(ASCE)1090-0241(2004)130:6(580).

Bai, Y. 2003. *Marine Structural Design*. Amsterdam: Elsevier.

Balestrini, F., D. Draganov, M. Staring, J. Singer, J. Heijmans, and P. Karamitopoulos. 2021. *Seismic Modelling for Monitoring of Historical Quay Walls and Detection of Failure Mechanisms*. Paper presented at the NSG2021 2nd Conference on Geophysics for Infrastructure Planning, Monitoring and BIM.

Bayes, T. 1763. "LII. An Essay Towards Solving a Problem in the Doctrine of Chances. By the Late Rev. Mr. Bayes, FRS Communicated by Mr. Price, in a Letter to John Canton, AMFR S." *Philosophical Transactions of the Royal Society of London* 53:370–418. https://doi.org/10.1098/rstl.1763.0053.

Beck, J. L., and S.-K. Au. 2002. "Bayesian Updating of Structural Models and Reliability Using Markov Chain Monte Carlo Simulation." *Journal of Engineering Mechanics* 128 (4): 380–391. https://doi.org/10.1061/(ASCE)0733-9399(2002)128:4(380).

Ching, J., H.-D. Lin, and M.-T. Yen. 2011. "Calibrating Resistance Factors of Single Bored Piles Based on Incomplete Load Test Results." *Journal of Engineering Mechanics* 137 (5): 309–323. https://doi.org/10.1061/(ASCE)EM.1943-7889.0000230.

Choe, D.-E., P. Gardoni, and D. Rosowsky. 2007. "Closed- form Fragility Estimates, Parameter Sensitivity, and Bayesian Updating for RC Columns." *Journal of Engineering Mechanics* 133 (7): 833–843. https://doi.org/10.1061/(ASCE)0733-9399(2007)133:7(833).

Choosrithong, K., and M. Korff. 2023. *Overamstel Project - Geotechnical Base report of Overamstel Project*. Openresearch, Amsterdam. https://openresearch.amsterdam/en/page/101481/geotechnical-base-report-of-overamstel-project.

Chung, T. H., Y. Mohamed, and S. AbouRizk. 2006. "Bayesian Updating Application Into Simulation in the North Edmonton Sanitary Trunk Tunnel Project." *Journal of Construction Engineering and Management* 132 (8): 882–894. https://doi.org/10.1061/(ASCE)0733-9364(2006)132:8(882).

Den Adel, N., J. De Gijt, H. Wolters, and T. Schweckendiek. 2019. *The Potential of Using Performance Information in the Assessment of Existing Quay Walls*. Paper presented at the IOP Conference Series: Materials Science and Engineering.

Deng, J. 2006. "Structural Reliability Analysis for Implicit Performance Function Using Radial Basis Function Network." *International Journal of Solids and Structures*

43 (11-12): 3255–3291. https://doi.org/10.1016/j.ijsolstr.2005.05.055.

Der Kiureghian, A., and O. Ditlevsen. 2009. "Aleatory or Epistemic? Does it Matter?" *Structural Safety* 31 (2): 105–112. https://doi.org/10.1016/j.strusafe.2008.06.020.

Ehre, M., I. Papaioannou, and D. Straub. 2018. "Efficient Conditional Reliability Updating with Sequential Importance Sampling." *Proceedings in Applied Mathematics and Mechanics.*

Enright, M. P., and D. M. Frangopol. 1999. "Condition Prediction of Deteriorating Concrete Bridges Using Bayesian Updating." *Journal of Structural Engineering* 125 (10): 1118–1125. https://doi.org/10.1061/(ASCE)0733-9445(1999)125:10(1118).

Farmaga, I., P. Shmigelskyi, P. Spiewak, and L. Ciupinski. 2011. *Evaluation of Computational Complexity of Finite Element Analysis.* Paper presented at the 2011 11th International Conference the Experience of Designing and Application of CAD Systems in Microelectronics (CADSM).

Gao, X., G. Duan, and C. Lan. 2021. "Bayesian Updates for an Extreme Value Distribution Model of Bridge Traffic Load Effect Based on SHM Data." *Sustainability* 13 (15): 8631. https://doi.org/10.3390/su13158631.

Hall, W. B. 1988. "Reliability of Service-Proven Structures." *Journal of Structural Engineering* 114 (3): 608–624. https://doi.org/10.1061/(ASCE)0733-9445(1988)114:3(608).

Hansen, J. B., and H. Lundgren. 1960. *Hauptprobleme der Bodenmechanik.* Berlin: Springer-Verlag .

Harmsen, L., and T. V. Nissen. 1965. "Timber Decay Caused by Bacteria." *Nature* 206 (4981): 319–319. https://doi.org/10.1038/206319a0.

Hemel, M. 2023. *Amsterdam Quays Under Pressure: Modelling and Testing of Historic Canal Walls.*

Hemel, M.-J., M. Korff, and D. J. Peters. 2022. "Analytical Model for Laterally Loaded Pile Groups in Layered Sloping Soil." *Marine Structures* 84:103229. https://doi.org/10.1016/j.marstruc.2022.103229.

Heming, S. 2019. *De Amsterdamse kademuren op de schop.* Van Hall Larenstein, Velp.

JCSS. 2000. "Probabilistic Model Code-Part 3." *Joint Committee on Structural Safety.*

Jiang, S.-H., D.-Q. Li, Z.-J. Cao, C.-B. Zhou, and K.-K. Phoon. 2015. "Efficient System Reliability Analysis of Slope Stability in Spatially Variable Soils Using Monte Carlo Simulation." *Journal of Geotechnical and Geoenvironmental Engineering* 141 (2): 04014096. https://doi.org/10.1061/(ASCE)GT.1943-5606.0001227.

Jonkman, S., R. Steenbergen, O. Morales-Nápoles, A. Vrouwenvelder, and J. Vrijling. 2015. "Probabilistic Design: Risk and Reliability Analysis in Civil Engineering." *Collegedictaat CIE4130.*

Kanning, W., and T. Schweckendiek. 2017. *Handreiking Faalkansanalyse en Faalkans Updating- Groene Versie - Macrostabiliteit Binnenwaarts.* helpdeskwater https://www.helpdeskwater.nl/onderwerpen/waterveiligheid/primaire/nieuwe-methoden-technieken/bewezen-sterkte/.

Kavitha, P., K. Beena, and K. Narayanan. 2016. "A Review on Soil–Structure Interaction Analysis of Laterally Loaded Piles." *Innovative Infrastructure Solutions* 1 (1): 1–15. https://doi.org/10.1007/s41062-016-0015-x.

Kim, S.-H., and M. Shinozuka. 2004. "Development of Fragility Curves of Bridges Retrofitted by Column Jacketing." *Probabilistic Engineering Mechanics* 19 (1-2): 105–112. https://doi.org/10.1016/j.probengmech.2003.11.009.

Kool, J., W. Kanning, C. Jommi, and S. N. Jonkman. 2021. "A Bayesian Hindcasting Method of Levee Failures Applied to the Breitenhagen Slope Failure." *Georisk: Assessment and Management of Risk for Engineered Systems and Geohazards* 15 (4): 299–316. https://doi.org/10.1080/17499518.2020.1815213.

Korff, M., M. Hemel, and R. Esposito. 2021. *Bezwijken Grimburgwal: Leerpunten voor het Amsterdamse Areaal.*

Korff, M., M.-J. Hemel, and D. J. Peters. 2022. "Collapse of the Grimburgwal, a Historic Quay in Amsterdam, the Netherlands." *Proceedings of the Institution of Civil Engineers - Forensic Engineering* 175 (4): 96–105. https://doi.org/10.1680/jfoen.21.00018.

Lesny, K. 2009. "Safety of Shallow Foundations–Limit State Design According to Eurocode 7 vs. Alternative Design Concepts." *Georisk* 3 (2): 97–105.

Li, D.-Q., F.-P. Zhang, Z.-J. Cao, W. Zhou, K.-K. Phoon, and C.-B. Zhou. 2015. "Efficient Reliability Updating of Slope Stability by Reweighting Failure Samples Generated by Monte Carlo Simulation." *Computers and Geotechnics* 69:588–600. https://doi.org/10.1016/j.compgeo.2015.06.017.

Lin, J., L. Zhang, C. Liao, J. Zhang, H. Yang, Z. Zhang, and W. Wang. 2023. "Probabilistic Calibration of the p-y Method Considering Model Uncertainty for Ultimate Limit State Design of Monopiles." *Georisk: Assessment and Management of Risk for Engineered Systems and Geohazards*, 1–19. https://doi.org/10.1080/17499518.2023.2285832.

Lou, M., H. Wang, X. Chen, and Y. Zhai. 2011. "Structure–Soil–Structure Interaction: Literature Review." *Soil Dynamics and Earthquake Engineering* 31 (12): 1724–1731. https://doi.org/10.1016/j.soildyn.2011.07.008.

NEN-EN9997-1. 2012. *Eurocode 7 - Geotechnical Design of Structures - Part 1: General Rules.* https://www.nen.nl/nen-9997-1-c1-2012-nl-170391.

Norris, G. M. 1986. *Theoretically Based BEF Laterally Loaded Pile Analysis.*

Pagella, G., G. Ravenshorst, W. Gard, and J. W. van de Kuilen. 2021. *Characterization and Assessment of the Mechanical Properties of Spruce Foundation Piles Retrieved from Bridges in Amsterdam.*

Pagella, G., G. Ravenshorst, W. Gard, and J. W. van de Kuilen. 2022. *Characterization and Assessment of the Mechanical Properties of Spruce Foundation Piles Retrieved from Bridges in Amsterdam.* Paper presented at the 4th International Conference on Timber Bridges Switzerland.

Papaioannou, I., and D. Straub. 2012. "Reliability Updating in Geotechnical Engineering Including Spatial Variability of Soil." *Computers and Geotechnics* 42:44–51. https://doi.org/10.1016/j.compgeo.2011.12.004.

Pol, J., W. Van Klaveren, W. Kanning, V. Van Beek, B. Robbins, and S. N. Jonkman. 2021. *Progression Rate of Backward Erosion Piping: Small Scale Experiments.* Paper presented at the 10th International Conference on Scour and Erosion (ICSE-10), Arlington, Virginia, USA.

Roubos, A. A., D. L. Allaix, T. Schweckendiek, R. D. Steenbergen, and S. N. Jonkman. 2020. "Time-dependent

Reliability Analysis of Service-Proven Quay Walls Subject to Corrosion-Induced Degradation." *Reliability Engineering & System Safety* 203:107085. https://doi.org/10.1016/j.ress.2020.107085.

Schweckendiek, T. 2010. "Reassessing Reliability Based on Survived Loads." *COASTAL ENGINEERING*, 2. https://repository.tudelft.nl/islandora/object/uuid:2569afed-b3f4-4427-85cd-d8cb0c49dbe5?collection = research.

Schweckendiek, T., and W. Kanning. 2016. *Reliability Updating for Slope Stability of Dikes: Approach with Fragility Curves (Background Report)*. Deltares, Delft.

Schweckendiek, T., M. Van Der Krogt, A. Teixeira, W. Kanning, R. Brinkman, and K. Rippi. 2017. "Reliability Updating with Survival Information for Dike Slope Stability Using Fragility Curves." *Geo-Risk* 2017: 494–503.

Schweckendiek, T., A. Vrouwenvelder, and E. Calle. 2014. "Updating Piping Reliability with Field Performance Observations." *Structural Safety* 47:13–23. https://doi.org/10.1016/j.strusafe.2013.10.002.

Spannenburg, T. 2020. *Timber Creep of Historic Urban Quay Walls: The Influence of Timber Creep on the Assessment of Inner-city Quay Walls*.

Steenbergen, R., A. Vrouwenvelder, and N. Scholten. 2012. *Veiligheidsfilosofie bestaande bouw*. toepassing en interpretatie NEN 8700.

Straub, D. 2011. "Reliability Updating with Equality Information." *Probabilistic Engineering Mechanics* 26 (2): 254–258. https://doi.org/10.1016/j.probengmech.2010.08.003.

Straub, D., and I. Papaioannou. 2015. "Bayesian Updating with Structural Reliability Methods." *Journal of Engineering Mechanics* 141 (3): 04014134. https://doi.org/10.1061/(ASCE)EM.1943-7889.0000839.

Tabarroki, M., J. Ching, K.-K. Phoon, and Y.-Z. Chen. 2022. "Mobilisation-based Characteristic Value of Shear Strength for Ultimate Limit States." *Georisk: Assessment and Management of Risk for Engineered Systems and Geohazards* 16 (3): 413–434. https://doi.org/10.1080/17499518.2020.1859121.

van de Kuilen, J. W., O. Beketova-Hummel, G. Pagella, G. Ravenshorst, and W. Gard. 2021. *An Integral Approach for the Assessment of Timber Pile Foundations*. Paper presented at the World Conference on Timber Engineering 2021, WCTE 2021.

Varossieau, W. 1949. *Opgegraven en aangetast hout uit biologisch oogpunt bezien*.

Wang, Y. 2011. "Reliability-Based Design of Spread Foundations by Monte Carlo Simulations." *Géotechnique* 61 (8): 677–685. https://doi.org/10.1680/geot.10.P.016.

Yu, Y., and C. Cai. 2019. "Prediction of Extreme Traffic Load Effects of Bridges Using Bayesian Method and Application to Bridge Condition Assessment." *Journal of Bridge Engineering* 24 (3): 04019003. https://doi.org/10.1061/(ASCE)BE.1943-5592.0001357.

Yuen, K.-V. 2010. *Bayesian Methods for Structural Dynamics and Civil Engineering*. Singapore: John Wiley & Sons.

Zhang, L. 2004. "Reliability Verification Using Proof Pile Load Tests." *Journal of Geotechnical and Geoenvironmental Engineering* 130 (11): 1203–1213. https://doi.org/10.1061/(ASCE)1090-0241(2004)130:11(1203).

Zhang, J., L. Zhang, and W. H. Tang. 2011. "Slope Reliability Analysis Considering Site-Specific Performance Information." *Journal of Geotechnical and Geoenvironmental Engineering* 137 (3): 227–238. https://doi.org/10.1061/(ASCE)GT.1943-5606.0000422.